Wearable EEG and Stand-Alone VR for Mobile Neurorehabilitation: A Cortical Comparison of Real, Virtual, and Simulated Upper-Limb Training

Ahmad Achkar[‡§], Omar Achkar[*§], George Zouridakis[†], and Kyu In Lee[*]
[*]Department of Information Science Technology, [†]Department of Engineering Technology,
University of Houston, Houston, Texas 77204
[‡]Department of Biomedical Sciences, Texas A&M University, College Station, Texas, 77840
Email: {oachkar, gzourida, klee48}@central.uh.edu, ahmadachkar@tamu.edu

***Abstract*—Upper-limb motor rehabilitation depends on intensive, high-repetition practice that is difficult to deliver outside the clinic. Immersive virtual reality (VR) is a promising substitute, but its value depends on whether the brain activity that drives motor recovery is preserved when patients practice with virtual rather than physical objects. To test this, we used electroencephalography (EEG) to record movement-related cortical potentials (MRCPs), the slow brain signals that precede voluntary movement and reflect motor preparation. Three participants performed an upper-limb reach-and-release task in three matched conditions, each for 150 trials: real object manipulation (RMT), VR with on-device hand tracking (VRMT), and object-free simulated movement (SMT). EEG was recorded with a wireless 24-channel wearable amplifier, and the VR headset and a webcam-based gesture detector were synchronized to it through the Lab Streaming Layer on a single host laptop. The peak motor potential (MP) component of the MRCP was closely matched at Cz between VRMT and RMT ($p = 0.95$) and significantly larger in VRMT than in SMT ($p = 0.041$). Within-session MP reductions consistent with motor learning emerged in the RMT ($p = 0.050$) and at trend level in the VRMT ($d = -1.41$), but were absent in the SMT. These proof-of-concept findings suggest that VR-based training engages cortical preparation networks comparably to physical practice, with implications for the design of mobile, EEG-guided rehabilitation systems.**

***Index Terms*—Wearable EEG, stand-alone virtual reality, mobile multimodal sensing, brain-computer interface, motor rehabilitation, upper-limb training.**

I. Introduction

Upper-limb motor impairments are among the most debilitating consequences of stroke and traumatic brain injury, affecting millions of individuals worldwide and driving sustained demand for effective, scalable rehabilitation approaches [1]. Traditional physical therapy relies on high-repetition, task-specific practice with real objects, and meta-regression evidence indicates a positive dose–response relationship between training dose and motor outcomes after stroke [2]; clinical constraints such as limited therapist availability, patient fatigue, and safety concerns in early recovery, however, often restrict the dosage that patients actually receive. These limitations have motivated growing interest in technology-assisted platforms that can deliver intensive, customizable motor practice outside the conventional therapy setting.

Electroencephalography (EEG) records cortical electrical activity through electrodes placed on the scalp, with millisecond temporal resolution. It is non-invasive, portable, and inexpensive relative to MRI or MEG, which has made it the standard modality for closed-loop motor brain-computer interfaces (BCIs) and for cortical instrumentation of motor rehabilitation outside the laboratory. Among the EEG signals relevant to motor function, movement-related cortical potentials (MRCPs) are slow negative shifts that begin up to 1.5 to 2 s before voluntary movement, reflecting cortical motor planning and initiation [3]. Their sensitivity to task complexity and skill level makes them valuable both as biomarkers of motor preparation and as indicators of training-related plasticity [4], [5]. MRCPs are also widely used as BCI control signals for assistive devices, where their detectability even without overt movement is a key advantage; combined with sensorimotor rhythm (mu/beta) desynchronization, they provide a rich characterization of how motor networks reorganize during rehabilitation [6].

Virtual reality (VR) has been studied as a stroke-rehabilitation platform. In a 2025 meta-analysis of 190 stroke trials, Laver et al. [7] reported that VR may slightly improve upper-limb function compared with alternative therapy and probably increases arm function when added to usual care. EEG evidence that VR engages motor-related cortical activity comes from a small number of clinical studies. Calabró et al. [8] reported, in a randomized trial of post-stroke gait rehabilitation, that robot-assisted training combined with VR produced larger event-related spectral perturbations and stronger cortical activations than robot-assisted training alone, alongside greater gains in mobility and balance. However, prior EEG studies of VR motor tasks have focused primarily on spectral (mu/beta) features or have been limited to two-condition designs (real vs. virtual, or real vs. imagined), leaving the slow cortical potentials that directly index motor planning largely unexplored in immersive VR contexts.

The hardware that could support such practice has shifted

[§]Ahmad Achkar and Omar Achkar contributed equally as co-first authors.

in the past few years. Stand-alone VR headsets such as the Meta Quest 3 include on-device cameras, inside-out tracking, and camera-based hand tracking with no external base stations, which removes the desktop-PC tether that defined earlier laboratory VR. Wireless multichannel EEG amplifiers transmit raw data over Bluetooth at sampling rates appropriate for cortical recording, decoupling EEG acquisition from a wired cabinet, and recent dry-contact and miniaturized electrode designs have extended this acquisition path toward fully wearable, in-the-wild deployments [9]. Open-source streaming infrastructure such as the Lab Streaming Layer (LSL) [10] coordinates clocks across these heterogeneous devices in software, so that a single edge laptop can ingest physiological, kinematic, and behavioral streams in real time. Together these developments make it conceivable to run an EEG-guided motor rehabilitation session entirely on commodity, mobile hardware, with the inference and feedback loop running on the patient's own machine rather than a clinic workstation. What none of this hardware progress addresses is whether the cortical activity that drives motor learning survives the move from physical practice to immersive VR. If MRCPs in VR look like those in a low-fidelity simulation rather than those in real movement, no amount of mobile-computing improvement makes the system therapeutically useful.

Despite the growing body of EEG work in VR, no study has directly compared MRCP components across three matched task formats: real, fully immersive VR, and object-free simulated movement. Without that comparison it is not possible to tell whether VR reproduces the cortical signatures of physical practice or behaves more like a low-fidelity simulation. Our paper addresses this gap through a within-subjects comparison of the Bereitschaftspotential (BP), negative slope (NS′), and motor potential (MP) recorded during a self-paced upper-limb reach-and-release task performed under all three conditions. These three components reflect successive stages of cortical motor preparation: the BP, generated chiefly by supplementary motor area, indexes early planning and the general intention to move; the NS′ tracks the transition from general intention to a specific motor program over premotor and contralateral motor cortex; and the MP, focal to contralateral primary motor cortex at movement onset, represents the cortical motor command itself [3]. Examining all three allows any cross-condition difference to be localized to a specific stage of preparation. By additionally examining within-session amplitude reductions as a marker of cortical-level learning, the study provides an initial assessment of how training environment shapes both the magnitude and plasticity of motor preparation activity relevant to neurorehabilitation.

This paper makes three contributions. First, it provides the first head-to-head comparison of MRCP components across real, fully immersive VR with hand tracking, and object-free simulated movement in the same participants, isolating the effect of training environment on cortical motor preparation. Second, it documents within-session amplitude reductions in the real and VR conditions but not the simulated condition, giving initial evidence that VR engages the same plasticity-related dynamics as physical practice. Third, the cortical findings are obtained on the kind of wearable, mobile hardware that could be deployed outside the laboratory, so they speak directly to the viability of that hardware path for EEG-guided rehabilitation.

II. Related Work

A. MRCPs and VR in motor rehabilitation

MRCPs are used to infer movement intention and drive BCIs for neurorehabilitation devices [6], [11], with case-study evidence that closed-loop BCI training combined with a robotic exoskeleton can support functional recovery in chronic stroke [12]. Wright et al. [5] showed that motor cortex activity during movement preparation is reduced after a period of skill practice, with smaller MRCP amplitudes interpreted as a neural-efficiency signature of motor learning. Jochumsen et al. [6] reported that MRCP components and sensorimotor EEG rhythms carry complementary discriminative information for trial-by-trial decoding of grasp type and grasp kinetics, with the combination of the two feature classes outperforming either alone. Olsen et al. [4] reviewed 59 studies of MRCPs in ecologically valid movements and noted that the literature has been dominated by simple single-joint tasks and is gradually moving toward multi-joint movements such as reach-to-grasp.

EEG evidence for VR engaging motor-related cortical activity comes from a small number of complementary studies. Calabró et al. [8] reported, in a randomized clinical trial of post-stroke gait rehabilitation, that robot-assisted therapy combined with VR produced larger event-related spectral perturbations and stronger cortical activations than robot-assisted therapy alone, alongside greater gains in mobility and balance. Lakshminarayanan et al. [13] found that combining VR-based action observation with kinesthetic motor imagery enhanced alpha and beta-band desynchronization beyond motor imagery alone. Direct head-to-head comparisons of the same motor task executed physically and in immersive VR, with slow cortical potentials as the dependent measure, are rare; existing EEG-and-VR studies have typically focused on spectral features or have used two-condition designs.

B. Comparing MRCPs across task formats

The most directly related prior work is Ogahara et al. [14], who compared MRCPs during real and simulated non-dominant hand object-dropping. The simulated condition produced smaller BP, NS′, and MP amplitudes and later onset times than the real condition, indicating that the absence of a physical object attenuates cortical motor preparation. Ogahara et al. did not include an immersive VR condition, leaving open whether VR with naturalistic hand tracking sits closer to the real or to the simulated end of that spectrum.

C. Positioning of the present study

The present work extends this literature by directly comparing MRCPs across three conditions (real, simulated, and

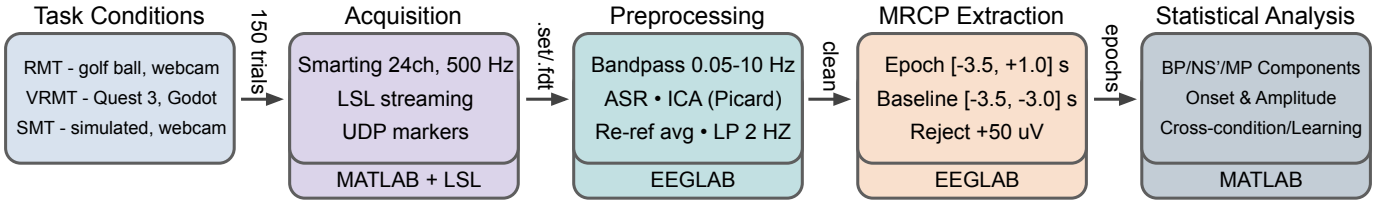

Fig. 1: Recording and analysis pipeline. EEG from the wireless amplifier and trial markers from the webcam (RMT, SMT) or the game engine (VRMT) are streamed over LSL to a host laptop and analyzed offline in EEGLAB.

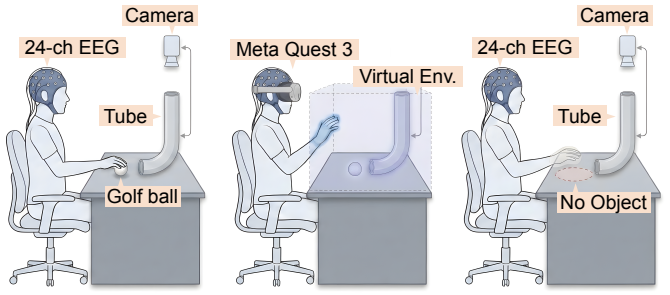

Fig. 2: Task conditions, side view. (a) RMT: real golf ball, overhead webcam. (b) VRMT: Godot scene on a Meta Quest 3S with on-device hand tracking. (c) SMT: same reach-and-release motion, no object.

immersive VR) using the same upper-limb task, with camera-based hand tracking to preserve natural kinematics. By examining early and late trial blocks, the design also captures learning-related MRCP dynamics. As a preliminary study with a small sample, the goal is to establish proof of concept and motivate adequately powered follow-up work.

III. Methods

This study used a within-subjects design in which each participant performed an upper-limb reach-and-release task under three matched conditions: real (RMT), VR with hand tracking (VRMT), and object-free simulated movement (SMT), with EEG recorded continuously. Fig. 1 summarizes the recording chain and the offline analysis steps.

A. Participants

Three right-handed adults aged 22 to 28 years (all male) with normal or corrected-to-normal vision and no history of neurological or psychiatric conditions participated in the study. The non-dominant (left) hand was used for the motor task, following standard self-paced MRCP practice. All participants gave informed consent, and the protocol was approved by the University of Houston Institutional Review Board (study ID STUDY00005734).

B. Task Conditions

We adapted the upper-limb reach-and-release paradigm from Ogahara et al. [14] and added an immersive VR condition. In all three conditions (Fig. 2), seated participants used their non-dominant (left) hand to reach toward a target, grasp it, lift it to a vertical tube at eye level, and release. Self-paced MRCP studies in healthy participants conventionally use the non-dominant hand because dominant-hand movements are highly automatized and tend to elicit reduced MRCP amplitudes, which would compress the signal range available for cross-condition comparison. The RMT used a real golf ball on the table, with an overhead webcam capturing the workspace and a return mechanism rolling the ball back between trials. The VRMT replaced the ball, table, and tube with a Godot scene rendered on the Meta Quest 3S in the same spatial layout, with object grasp and release driven by the headset's on-device hand tracking rather than controllers. The SMT used the same physical workspace as the RMT but with no object present, so participants performed the same trajectory in empty space. The only systematic difference between the SMT and the RMT was therefore the presence of an object to be manipulated.

Participants were instructed to fix their gaze on the tube opening to minimize ocular artifacts, to maintain upright posture with minimal extraneous body movements, and to initiate each trial once they felt settled and ready, per standard self-paced MRCP protocols. Each condition consisted of 150 self-paced trials in six blocks of 25, with about 60 s of rest between blocks and a 10-minute rest period between conditions, and a minimum five-second inter-trial interval to preserve the pre-movement baseline. Conditions were administered in a fixed order (RMT, VRMT, SMT), yielding 450 trials per participant.

C. Acquisition

The recording chain combined a wearable EEG amplifier, a stand-alone VR headset, and a desktop webcam, all exchanging data with a single host laptop in real time (Fig. 3(a)). EEG was acquired with a 24-channel mBrainTrain Smarting wireless amplifier (Smart Pack; mBrainTrain) [15], fitted to an EasyCap RBE 24-channel research cap with gel-based electrodes (EasyCap GmbH) [16]. Electrodes covered frontal, central, temporal, parietal, occipital, and auxiliary sites per the international 10–20 system (Fig. 3(a)), with mastoid channels for reference and a common-mode-sense / driven-right-leg (CMS/DRL) configuration at the device. Data were sampled at 500 Hz and streamed continuously over Bluetooth via the Lab Streaming Layer (LSL) protocol [10] to the host laptop, which ran custom MATLAB acquisition software.

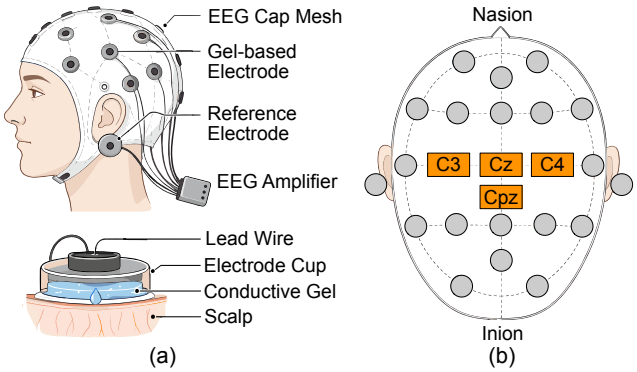

Fig. 3: EEG acquisition setup and analysis channels. (a) Wireless amplifier and gel-based electrodes mounted in a 10–20 cap, with a zoomed view of the electrode-scalp contact. (b) Electrode layout with the four analysis channels (C3, Cz, C4, CPz) highlighted.

The VR scene was implemented in the Godot 4.3 game engine [17] on the OpenXR runtime [18] and ran on a standalone Meta Quest 3S worn over the EEG cap. Hand tracking was performed entirely on-device using the headset's cameras, allowing controller-free interaction with a virtual ball, table, and tube laid out as in the real workstation; the game engine emitted PICKUP and DROP markers directly from virtual-object grasp and release events. For the RMT and SMT, an overhead camera observed the physical workspace, and a custom Python pipeline using OpenCV [19] emitted PICKUP and DROP markers when a per-user-calibrated finger-thumb distance crossed threshold in either direction.

All event markers, whether from the webcam pipeline or from the game engine, were transmitted to the recording laptop over UDP and timestamped on arrival against the LSL unified clock. Marker-to-EEG alignment was performed by direct sample indexing at the time of marker reception, yielding an end-to-end synchronization precision of approximately 50 ms, dominated by the software polling interval and well within the hundreds-of-milliseconds timescale of the MRCP components of interest. We additionally applied cross-correlation-based latency alignment during preprocessing to refine marker-to-EEG correspondence per trial.

D. Preprocessing

Offline preprocessing was performed in MATLAB using the EEGLAB toolbox [20]. The continuous EEG was bandpassed with a zero-phase Butterworth filter (order 4, 0.05 to 10 Hz) to remove slow drifts and high-frequency noise while preserving the slow cortical shifts that span seconds before movement. We then applied Artifact Subspace Reconstruction (ASR) via the `clean_rawdata` plugin with a burst threshold of $k = 30$ standard deviations (set conservatively to avoid clipping slow cortical shifts), a five-second flatline threshold, a channel correlation threshold of 0.7, and a line-noise criterion of four standard deviations. Window-based rejection was disabled so all time segments were retained for epoching.

Independent component analysis was run with the Picard algorithm [21] and automatic rank reduction. Components were classified with ICLabel [22], and any component whose summed probability across artifact categories (muscle, eye, heart, line noise, channel noise) exceeded 70% was removed. Channels rejected by ASR were restored by spherical interpolation, the data were re-referenced to the common average, and a second zero-phase low-pass at 2 Hz isolated the slow cortical band. A current source density (CSD) transform using the spherical-spline surface Laplacian was applied to sharpen spatial resolution. All amplitude values reported below are in μV/cm^2.

E. MRCP Extraction

Continuous data were epoched around the PICKUP marker. Because this marker corresponded to the moment of object contact rather than the onset of reaching, a 0.6 s trigger offset was applied to approximate movement initiation, yielding $[-3.5, +1.0]$ s epochs relative to estimated onset. Baseline correction subtracted the mean amplitude over the pre-movement reference window $[t_{b1}, t_{b2}] = [-3.5, -3.0]$ s:

$$x_i^{\mathrm{bc}}(t) = x_i(t) - \frac{1}{T_b} \sum_{t'=t_{b1}}^{t_{b2}} x_i(t'). \tag{1}$$

Epochs exceeding ± 50 μV on any channel were rejected, and we applied additional statistical rejection by joint probability and kurtosis (five-SD threshold). Remaining clean trials were averaged per condition c and participant p:

$$\bar{x}_i^{(c,p)}(t) = \frac{1}{N_{\mathrm{clean}}} \sum_{n=1}^{N_{\mathrm{clean}}} x_{i,n}^{(c,p)}(t). \tag{2}$$

We extracted three MRCP components at C3, Cz, C4, and CPz (Fig. 3(b)), chosen because MRCPs are maximal over the vertex and sensorimotor cortex overlying the hand area [3]. At Cz, the BP was the mean amplitude on $[-2.6, -1.1]$ s,

$$\mathrm{BP} = \frac{1}{T_{\mathrm{BP}}} \int_{-2.6}^{-1.1} x_{\mathrm{Cz}}(t)\, dt; \tag{3}$$

the NS$'$ was the mean amplitude on $[-1.1, -0.6]$ s,

$$\mathrm{NS}' = \frac{1}{T_{\mathrm{NS}'}} \int_{-1.1}^{-0.6} x_{\mathrm{Cz}}(t)\, dt; \tag{4}$$

and the MP was the peak negative amplitude on $[-2.6, -0.6]$ s,

$$\mathrm{MP} = \min_{t \in [-2.6, -0.6]} x_{\mathrm{Cz}}(t). \tag{5}$$

BP and NS$'$ onset latencies were obtained by backward search with amplitude thresholds of -1.0 μV/cm^2 and -2.5 μV/cm^2, respectively. To probe within-session learning, we split each participant's trials into early (first 60) and late (last 60) subsets and compared component measures across the two halves.

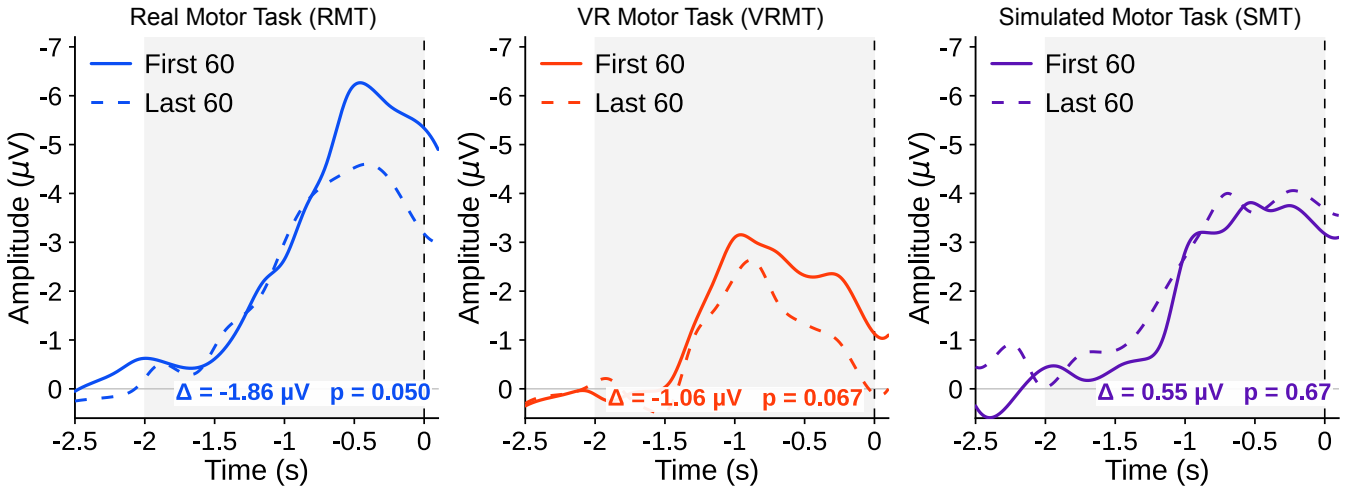

Fig. 4: Within-session learning at Cz. First 60 (solid) vs. last 60 (dashed) trials in each condition. Movement onset at $t = 0$.

F. Statistical Analysis

All statistical comparisons used paired t-tests on per-participant means. We compared MRCP component amplitudes and onset latencies across conditions at Cz, and component amplitudes between the first 60 and last 60 trials within each condition for the within-session learning analysis. One-tailed tests were used for directional contrasts motivated by prior work (VRMT $>$ SMT and RMT $>$ SMT for amplitudes; first $>$ last block for within-session reductions) and two-tailed tests for the VRMT-vs.-RMT contrast, where no a priori direction had been specified. All reported p-values are uncorrected for multiple comparisons; given the exploratory aim of the study and the small sample, all results should be read accordingly. Effect sizes are reported as Cohen's d.

IV. Results

A. MRCP morphology across conditions

Each of the three conditions produced a recognizable MRCP at the central electrode sites (Fig. 4, which shows the grand-average waveforms at Cz). In every condition the waveform began with a gradual negative shift approximately 2 s before movement onset and reached peak negativity near the time of object contact, matching the morphology reported for self-paced MRCP paradigms. The three MRCP components defined in Section III-E were all extractable in every condition and at all four analysis channels (C3, Cz, C4, and CPz, the central scalp positions over sensorimotor cortex where MRCPs are typically maximal): the early Bereitschaftspotential (BP, motor planning), the late negative slope (NS′, motor programming), and the peak motor potential (MP, the cortical motor command). At Cz, the grand-average MP amplitudes were -3.91 μV/cm^2 in the RMT, -3.97 μV/cm^2 in the VRMT, and -2.95 μV/cm^2 in the SMT; these are the bar heights plotted in Fig. 5(a). The self-paced reach-and-release task therefore elicited MRCPs reliably across all three task formats, and the MP component was visibly larger in the two object-interaction conditions than in the object-free condition. Formal cross-condition comparisons follow.

B. Cross-condition comparisons

The MP amplitude comparison at Cz is summarized in Fig. 5(a) and the corresponding scalp distributions in Fig. 5(b); BP, NS′, and onset values are reported numerically below.

The headline finding is that the VRMT and RMT produced equivalent MP amplitudes at Cz (Fig. 5(a)). The paired comparison was not significant ($t(2) = 0.07$, $p = 0.95$, two-tailed, $d = 0.04$), indicating that immersive VR with on-device hand tracking engages cortical motor preparation at the same magnitude as physical object manipulation, even without true tactile or weight feedback. The scalp distributions in Fig. 5(b) mirror this amplitude match: both RMT and VRMT show vertex-focused negativity centered near Cz, consistent with a common sensorimotor generator. The NS′ amplitude showed a trend-level difference in the opposite direction, with the RMT eliciting more negative mean amplitudes than the VRMT during the late preparation window ($t(2) = -3.36$, $p = 0.078$, two-tailed, $d = -1.94$). The large NS′ effect size combined with the matched MP suggests that physical grasping recruits additional sustained negativity in the seconds approaching object contact, possibly reflecting somatosensory anticipation, while the peak motor command itself reaches the same amplitude in VR.

By contrast, the VRMT produced significantly larger MP amplitudes than the SMT (Fig. 5(a)). The paired comparison was significant ($t(2) = -3.29$, $p = 0.041$, one-tailed, $d = -1.90$), placing immersive VR closer to the real-object end of the spectrum than to object-free imagined movement. The implication is that what drives cortical motor engagement in this paradigm is not the physicality of the object but the presence of a target to act on: replacing the golf ball with a virtual ball preserves cortical recruitment, while removing the object entirely attenuates it. The scalp distribution for the SMT (Fig. 5(b)) is correspondingly more diffuse than

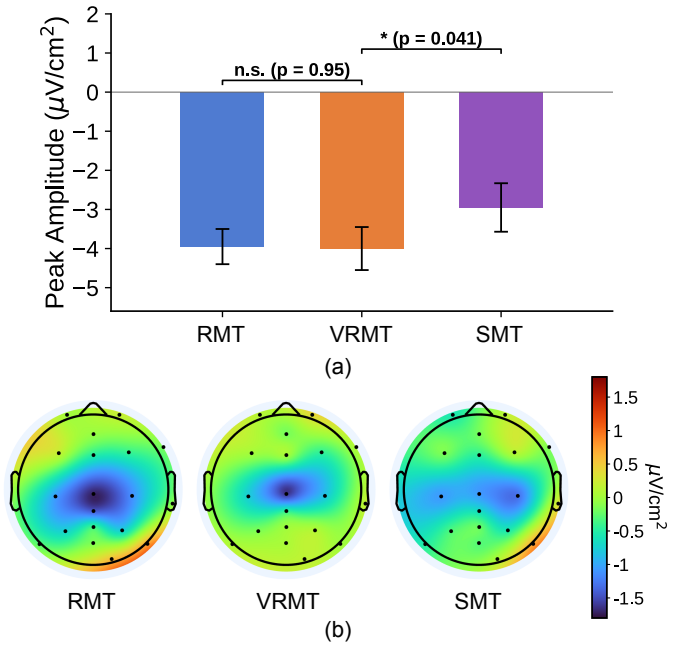

Fig. 5: Cross-condition MP amplitude at Cz and scalp distribution. (a) Peak MP amplitude across conditions with standard error bars. (b) Current source density scalp topographies for RMT, VRMT, and SMT.

the two object-interaction conditions, with less focal vertex negativity. NS′ amplitude did not differ significantly between VRMT and SMT, and the observed direction was opposite to the directional prediction ($t(2) = 1.47$, $p = 0.28$, two-tailed, $d = 0.85$); given the small sample, this NS′ contrast is best read as not yet interpretable. For the RMT-vs.-SMT contrast, BP amplitude showed a trend-level reduction in the SMT ($t(2) = -2.24$, $p = 0.077$, one-tailed, $d = -1.29$), echoing the same object-presence effect at the early planning stage of the MRCP.

Onset latencies indicate that motor preparation began earlier in the RMT than in the VRMT. BP onset was at -1.32 s relative to movement in the RMT and -0.71 s in the VRMT ($t(1) = -22.46$, $p = 0.014$, one-tailed). BP onset was detectable in both conditions for only 2 of 3 participants, so this contrast carries a single degree of freedom and should be interpreted with caution. NS′ onset showed a similar but non-significant trend toward an earlier onset in the RMT ($t(2) = -1.93$, $p = 0.096$, one-tailed, $d = -1.12$). Combined with the matched peak MP amplitude between VRMT and RMT, these latency results suggest that VR engages the same final motor-preparation networks as physical practice, but takes longer to initiate the planning phase. A plausible reading is that participants need more time to bind the virtual hand to the rendered scene before committing to action, while the recruited cortical machinery is otherwise the same.

C. Within-session learning

To test whether the three task formats supported within-session motor learning at the cortical level, we split each participant's trials into early (first 60) and late (last 60) subsets and compared MRCP component amplitudes between the two subsets with paired t-tests. We quantified learning-related amplitude reduction as the late-minus-early difference, where a more negative early block indicates greater cortical engagement during initial practice, consistent with a neural-efficiency interpretation of motor learning. Fig. 4 shows the grand-average waveforms for the first and last trial blocks at Cz.

The RMT showed clear amplitude reductions across the session. At Cz, the NS′ amplitude reduction was non-significant ($\Delta = -1.37$ μV/cm^2, $t(2) = -1.60$, $p = 0.126$, one-tailed, $d = -0.92$), with a comparable non-significant reduction at CPz ($\Delta = -0.96$ μV/cm^2, $t(2) = -1.75$, $p = 0.111$, one-tailed, $d = -1.01$). The MP amplitude reduction reached significance at both sites (Cz: $\Delta = -1.86$ μV/cm^2, $t(2) = -2.93$, $p = 0.050$, one-tailed, $d = -1.69$; CPz: $\Delta = -1.29$ μV/cm^2, $t(2) = -3.13$, $p = 0.044$, one-tailed, $d = -1.81$).

The VRMT produced a qualitatively similar pattern. At Cz, the NS′ amplitude showed a non-significant trend toward reduction ($\Delta = -1.09$ μV/cm^2, $t(2) = -1.18$, $p = 0.179$, one-tailed, $d = -0.68$), and the MP amplitude showed the same direction at trend level ($\Delta = -1.06$ μV/cm^2, $t(2) = -2.44$, $p = 0.067$, one-tailed, $d = -1.41$). The MP effect size in the VRMT was large ($d = -1.41$), so the trend-level p-value plausibly reflects a genuine learning effect that is attenuated by the small sample size rather than an absence of cortical plasticity during VR practice.

By contrast, the SMT showed no evidence of within-session amplitude change. All comparisons returned non-significant p-values with small effect sizes in the opposite, amplitude-increasing direction (all $p > 0.50$, $d \approx 0.3$), indicating that object-free simulated movement did not produce measurable within-session plasticity at the cortical level.

V. Discussion

A. VR reproduces cortical motor preparation signatures

The principal observation of this study is that MRCP amplitudes recorded during immersive VR upper-limb training closely resembled those recorded during equivalent physical movement. At Cz, the VRMT and RMT produced closely matched MP amplitudes ($p = 0.95$, two-tailed), with the VRMT eliciting a peak negativity of -3.97 μV/cm^2 compared to -3.91 μV/cm^2 for the RMT. The NS′ amplitude showed a trend-level difference ($p = 0.078$, two-tailed, $d = -1.94$), with the RMT producing more sustained negativity in the late preparation window, possibly reflecting somatosensory anticipation that VR cannot reproduce. By contrast, the SMT produced significantly attenuated MRCPs at the same site (-2.95 μV/cm^2; $p = 0.041$ vs. VRMT, uncorrected). These results provide initial evidence that immersive VR with camera-based hand tracking can engage cortical motor preparation networks at a level comparable to physical object manipulation and substantially above object-free simulated movement. Given the small sample size ($n = 3$), the absence

of a significant VRMT-vs.-RMT difference should be read as suggestive rather than as formal evidence of equivalence; a dedicated equivalence test with a larger sample would be required for that.

This finding extends prior VR-EEG work, which has so far focused on spectral features. Wang et al. [23] characterized neural oscillations during full-body reaching in 3D VR, and Calabró et al. [8] reported stronger event-related spectral perturbations during VR-augmented gait training than during robot-assisted training alone. The present results show that the MRCPs themselves, which directly index motor planning and the eventual motor command, are also preserved in immersive VR. Camera-based hand tracking rather than controllers likely contributed to this correspondence, since it preserves the hand kinematics and reach trajectory of the physical task.

B. VR supports within-session neural plasticity

A central question for VR-based neurorehabilitation is whether practice in VR produces genuine cortical-level plasticity or merely engages motor networks in a static manner. The present results favor the former interpretation, though they should be considered preliminary given the sample size and design constraints. Within-session amplitude reduction is a recognized cortical signature of motor learning [5], and it was observed not only during the RMT but also during the VRMT. The VRMT learning effects at Cz ($d = -0.68$ to -1.41) were qualitatively similar in direction to those seen in the RMT ($d = -0.92$ to -1.69), suggesting that VR practice may produce cortical efficiency gains comparable in direction to those elicited by physical practice, though the NS′ effect sizes in the VRMT were moderate rather than large. Because the condition order was fixed (RMT $\rightarrow$ VRMT $\rightarrow$ SMT), the amplitude reductions observed in the VRMT could partially reflect continued task familiarization carried over from the preceding RMT block; counterbalanced designs will be needed to isolate VR-specific plasticity from generic learning of the reach-and-release motion.

The absence of any learning effect in the SMT ($d \approx 0.3$, opposite direction) strengthens this interpretation. Ogahara et al. [14] previously documented attenuated MRCP amplitudes in simulated relative to real movement, and the present data replicate that amplitude pattern while extending it to an immersive VR condition. The dissociation across conditions suggests that the critical factor for cortical-level learning is not movement per se but the presence of a goal object, whether physical or virtual, that engages the complete motor planning sequence from target identification through grasp execution.

These observations are encouraging for neurorehabilitation. If confirmed in larger samples, the finding that VR-based motor training produces cortical plasticity signals comparable to physical practice would support VR as a viable complement to physical therapy in settings where real-world object manipulation is impractical, such as early post-stroke rehabilitation when patients cannot yet safely handle physical objects [7].

C. BP onset latency: early planning versus final execution

Despite the close match in MRCP amplitudes between the VRMT and RMT, the RMT exhibited an earlier BP onset than the VRMT (-1.32 s vs. -0.71 s before movement; $t(1) = -22.46$, $p = 0.014$, one-tailed; BP onset detectable in 2 of 3 participants). Although this contrast is based on only two participants and should be treated cautiously, the pattern, if confirmed, would suggest that physical object interaction recruits supplementary motor area and premotor cortex earlier in the planning sequence, possibly because the brain begins preparing for anticipated object weight, texture, and haptic feedback before the hand has reached the object [3]. The absence of these physical properties in VR may delay the initial recruitment of preparatory networks without diminishing their eventual engagement, as reflected in the closely matched peak MP amplitudes.

This dissociation between early planning and final command has practical relevance for BCI design. MRCP-based BCIs that rely on detecting the early BP component may face reduced detection windows during VR-based interaction and require adjusted detection thresholds, whereas BCIs targeting the later NS′ or MP components should perform comparably across real and virtual environments [11].

D. Implications for rehabilitation system design

Three design implications follow for VR-based neurorehabilitation systems intended to operate outside the laboratory. First, immersive VR with naturalistic hand tracking can engage cortical preparation networks at levels approaching those of physical movement; combined with a wireless wearable EEG amplifier and a stand-alone VR headset, the same hardware footprint plausibly extends to home or low-resource clinical settings. Second, the within-session cortical amplitude changes during VR practice indicate that MRCPs are a candidate real-time biomarker for adaptive, BCI-guided protocols in which task difficulty tracks the state of the user's motor preparation networks; meta-analytic evidence supports the broader effectiveness of BCI-based motor rehabilitation in stroke [24]. Third, the failure of object-free simulation to engage these networks, combined with prior work showing that motor transfer requires matched kinematic and spatial constraints [25], underscores the importance of goal-directed object interaction in VR rehabilitation design, even when the object is virtual.

E. Limitations and next steps

This study is best understood as proof-of-concept work. The sample of three participants, while sufficient to surface large within-condition effect sizes, limits statistical power and generalizability, and all reported p-values are uncorrected for multiple comparisons. The fixed condition order (RMT $\rightarrow$ VRMT $\rightarrow$ SMT) introduces potential practice-order and carryover confounds, particularly relevant to the within-session learning analysis in the VRMT. The 0.6 s trigger offset used to approximate movement onset was estimated rather than measured directly from behavioral data and may differ across

conditions, since the lag between pickup-event detection and actual movement onset depends on factors specific to each modality (camera framerate and finger-thumb threshold crossing for the webcam pipeline; virtual-object collision detection inside the game engine for VR). Future work should include a larger sample with counterbalanced condition order, independent movement-onset validation by accelerometry or motion capture, recording in clinical populations with motor impairments, and multi-session longitudinal designs to track plasticity beyond a single session. The integration of real-time MRCP decoding with adaptive VR task difficulty is a particularly promising next direction for closed-loop neurorehabilitation, since the wearable EEG and stand-alone VR substrate used here already supports the latency and synchronization budget that such a closed loop would require.

VI. Conclusion

This preliminary study presents the first direct three-way comparison of MRCPs recorded during real, virtual reality, and object-free simulated upper-limb training in the same participants. Immersive VR with camera-based hand tracking produced MRCP amplitudes closely matching those of physical movement at Cz and significantly larger than those of object-free simulation. Both the RMT and VRMT exhibited within-session amplitude reductions consistent with cortical-level motor learning, a pattern absent in the SMT. These proof-of-concept findings suggest that VR-based motor training can engage cortical preparation networks at a level comparable to physical practice, supporting its potential as a neurophysiologically grounded platform for upper-limb neurorehabilitation. The dissociation between VR and object-free simulated movement further highlights the importance of goal-directed object interaction for engaging cortical motor learning mechanisms, even when the object itself is virtual. The combination of wearable EEG and a stand-alone VR headset that produced these signals is the same hardware that would be deployed outside the laboratory, which makes the cortical results directly relevant to mobile, EEG-guided rehabilitation systems. Replication with larger samples, counterbalanced designs, and clinical populations is the essential next step.

Acknowledgments

The study was approved by the University of Houston Institutional Review Board (study ID STUDY00005734).

References

[1] L. Zhang, H. Lü, and C. Yang, "Global, regional, and national burden of stroke from 1990 to 2019: A temporal trend analysis based on the Global Burden of Disease Study 2019," *International Journal of Stroke*, vol. 19, no. 6, pp. 686–694, 2024.

[2] L. A. Boyd, C. E. Lang, and K. R. Lohse, "Is more better? using metadata to explore dose–response relationships in stroke rehabilitation," *Stroke*, vol. 45, no. 7, pp. 2053–2058, 2014.

[3] H. Shibasaki and M. Hallett, "What is the bereitschaftspotential?" *Clinical Neurophysiology*, vol. 117, no. 11, pp. 2341–2356, 2006.

[4] S. Olsen, G. Alder, M. Williams, S. Chambers, M. Jochumsen, N. Signal, U. Rashid, I. K. Niazi, and D. Taylor, "Electroencephalographic recording of the movement-related cortical potential in ecologically valid movements: A scoping review," *Frontiers in Neuroscience*, vol. 15, p. 721387, 2021.

[5] D. J. Wright, P. Holmes, F. Di Russo, M. Loporto, and D. Smith, "Reduced motor cortex activity during movement preparation following a period of motor skill practice," *PLoS ONE*, vol. 7, no. 12, p. e51886, 2012.

[6] M. Jochumsen, C. Rovsing, H. Rovsing, I. K. Niazi, K. Dremstrup, and E. N. Kamavuako, "Classification of hand grasp kinetics and types using movement-related cortical potentials and eeg rhythms," *Computational intelligence and neuroscience*, vol. 2017, no. 1, p. 7470864, 2017.

[7] K. E. Laver, B. Lange, S. George, J. E. Deutsch, G. Saposnik, M. Chapman, and M. Crotty, "Virtual reality for stroke rehabilitation," *Cochrane Database of Systematic Reviews*, no. 6, 2025.

[8] R. S. Calabrò, A. Naro, M. Russo, A. Leo, R. De Luca, T. Balletta, A. Buda, G. La Rosa, A. Bramanti, and P. Bramanti, "The role of virtual reality in improving motor performance as revealed by eeg: a randomized clinical trial," *Journal of neuroengineering and rehabilitation*, vol. 14, no. 1, p. 53, 2017.

[9] S. L. Kappel, M. L. Rank, H. O. Toft, M. R. Andersen, and P. Kidmose, "Dry-contact electrode ear-EEG," *IEEE Transactions on Biomedical Engineering*, vol. 66, no. 1, pp. 150–158, 2019.

[10] C. Kothe, S. Y. Shirazi, T. Stenner, D. Medine, C. Boulay, M. I. Grivich, F. Artoni, T. Mullen, A. Delorme, and S. Makeig, "The lab streaming layer for synchronized multimodal recording," *Imaging Neuroscience*, vol. 3, p. IMAG.a.136, 2025.

[11] H. Li, H. Shin, L. Sentis, K.-C. Siu, J. d. R. Millán, and N. Lu, "Combining vr with electroencephalography as a frontier of brain-computer interfaces," *Device*, vol. 2, no. 6, 2024.

[12] A. A. Frolov, P. Bobrov, E. V. Biryukova, I. Sirotkina, S. Kotov, L. G. Turbina, and A. Kondur, "Electrical, hemodynamic, and motor activity in BCI post-stroke rehabilitation: Clinical case study," *Frontiers in Neurology*, vol. 9, p. 1135, 2018.

[13] K. Lakshminarayanan, R. Shah, S. R. Daulat, V. Moodley, Y. Yao, and D. Madathil, "The effect of combining action observation in virtual reality with kinesthetic motor imagery on cortical activity," *Frontiers in Neuroscience*, vol. 17, p. 1201865, 2023.

[14] K. Ogahara, A. Nakashima, T. Suzuki, K. Sugawara, N. Yoshida, A. Hatta, T. Moriuchi, and T. Higashi, "Comparing movement-related cortical potential between real and simulated movement tasks from an ecological validity perspective," *Frontiers in Human Neuroscience*, vol. 17, p. 1313835, 2023.

[15] mBrainTrain LLC, "Smarting wireless EEG amplifier (smart pack)," https://mbraintrain.com/, Belgrade, Serbia, 2025.

[16] EasyCap GmbH, "EasyCap rbe 24-channel research EEG cap," https://www.easycap.de/, Etterschlag, Germany, 2025.

[17] Godot Foundation, "Godot engine," https://https://godotengine.org/, 2025.

[18] Khronos Group, "OpenXR specification," https://www.khronos.org/openxr/, 2019.

[19] G. Bradski, "The OpenCV library," *Dr. Dobb's Journal of Software Tools*, 2000.

[20] A. Delorme and S. Makeig, "EEGLAB: an open source toolbox for analysis of single-trial EEG dynamics including independent component analysis," *Journal of Neuroscience Methods*, vol. 134, no. 1, pp. 9–21, 2004.

[21] P. Ablin, J.-F. Cardoso, and A. Gramfort, "Faster independent component analysis by preconditioning with Hessian approximations," *IEEE Transactions on Signal Processing*, vol. 66, no. 15, pp. 4040–4049, 2018.

[22] L. Pion-Tonachini, K. Kreutz-Delgado, and S. Makeig, "ICLabel: An automated electroencephalographic independent component classifier, dataset, and website," *NeuroImage*, vol. 198, pp. 181–197, 2019.

[23] W.-E. Wang, R. L. Ho, B. Gatto, S. M. Van Der Veen, M. K. Underation, J. S. Thomas, A. B. Antony, and S. A. Coombes, "A novel method to understand neural oscillations during full-body reaching: a combined eeg and 3d virtual reality study," *IEEE transactions on neural systems and rehabilitation engineering*, vol. 28, no. 12, pp. 3074–3082, 2020.

[24] M. A. Cervera, S. R. Soekadar, J. Ushiba, J. d. R. Millán, M. Liu, N. Birbaumer, and G. Garipelli, "Brain-computer interfaces for post-stroke motor rehabilitation: a meta-analysis," *Annals of Clinical and Translational Neurology*, vol. 5, no. 5, pp. 651–663, 2018.

[25] D. E. Levac, M. E. Huber, and D. Sternad, "Learning and transfer of complex motor skills in virtual reality: a perspective review," *Journal of NeuroEngineering and Rehabilitation*, vol. 16, p. 121, 2019.